

Comparison of Four-Switch Buck-Boost and Dual Active Bridge Converter for DC Microgrid Applications

1st Ömer Ekin 

*Institute for Automation
and Applied Informatics (IAI)
Karlsruhe Institute of Technology (KIT)
Karlsruhe, Germany*

2nd Gabriele Arena 

*Institute for Technical Physics (ITEP)
Karlsruhe Institute of Technology (KIT)
Karlsruhe, Germany*

3rd Simon Waczowicz 

*Institute for Automation
and Applied Informatics (IAI)
Karlsruhe Institute of Technology (KIT)
Karlsruhe, Germany*

4th Veit Hagenmeyer 

*Institute for Automation and Applied Informatics (IAI)
Karlsruhe Institute of Technology (KIT)
Karlsruhe, Germany*

5th Giovanni De Carne 

*Institute for Technical Physics (ITEP)
Karlsruhe Institute of Technology (KIT)
Karlsruhe, Germany*

Abstract—Attention to DC Microgrids is recently increasing, due to the expansion of DC components, such as renewable energy sources (RESs), energy storage systems (ESSs), and DC loads. There is a large number of scientific publications on different converter topologies, but only a few of them addresses a direct comparison of different DC/DC converter solution for Microgrid applications. This work presents a comparison between Four-Switch Buck-Boost and Dual Active Bridge Converters in terms of applicability to DC Microgrids, considering efficiency and short circuit behavior.

Index Terms—DC-DC Converter, Four-Switch Buck-Boost, Dual Active Bridge, Converter Comparison, Microgrid

I. INTRODUCTION

The planned shift from fossil power generation to large-scale power plants, such as nuclear and coal-fired power plants, to renewable power generation results in a volatile power generation profile that is uncorrelated to the power demand profile, in addition to actor diversity. Microgrids are a promising concept for handling the associated complexity of energy management. Renewable energy sources in low voltage grids are usually direct current (DC) technologies and therefore need to be connected to the public power grid through a power converter. The fact that electricity storage systems and the vast majority of electricity consumers also use direct current has brought DC Microgrids into the focus of research. Within these DC Microgrids, a large number of conversions (from alternating current to direct current and vice versa) can be avoided, resulting in more efficient use of

electricity. Moreover, DC cables are not affected by the skin effect, which allows reducing size and cost of cables and DC Microgrids do not need synchronization of RESs or reactive power control. Since different components operate at different voltage levels, DC-DC converters are essential components for DC Microgrids [1], [2].

There is a wide variety of DC-DC converters available [3]. Among them, two very promising bidirectional up and down converters are the Four-Switch Buck-Boost (FSBB) converter and the Dual Active Bridge (DAB) converter. The FSBB converter is usually used in telecommunication and photovoltaic applications, whereas the DAB converter is more common for automotive applications such as on-board and off-board battery chargers, and for DC Microgrids as an interface with energy storage systems or to realize solid-state transformers (SSTs) [4]–[9]. In the present paper, the two converter technologies will be compared concerning their suitability for DC Microgrids. The focus here will be on the efficiency and safety of these converter technologies. For high-voltage DC (HVDC) and medium-voltage DC (MVDC) Microgrids, a comparison of modular multilevel converters (MMC) and DAB converters have been already done [10], but there is no similar comparison for FSBB and DAB in low voltage DC Microgrid applications, which is the goal of the present work. Even though it is important for the choice of converters, a comparison with regard to cost, size, and reliability is not part of this paper. The focus of the investigations is on the technical suitability for DC Microgrids. Special cases are also left out, where the possibilities of the FSBB are exhausted, such as very large gain factors between low and high voltage sides.

The present work is organized as follows: section II describes the studied DC-DC converters and the considered converter losses. In section III the short circuit behavior of both

This work was supported by the Helmholtz Association under the program "Energy System Design". The work of Giovanni De Carne was supported by the Helmholtz Association within the Helmholtz Young Investigator Group "Hybrid Networks" (VH-NG-1613). This project has also received funding from the European Union's Framework Programme for Research and Innovation, Horizon 2020 (2014–2020), under the Marie Skłodowska-Curie Grant Agreement No. 955614.

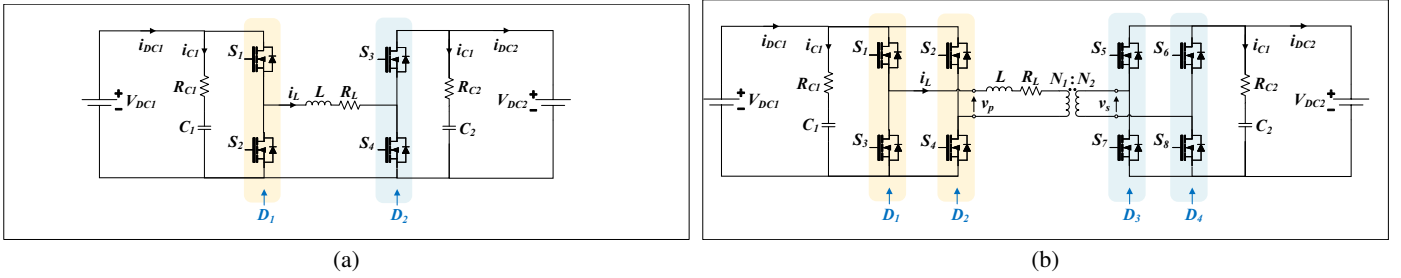


Fig. 1: Converter Topology: (a) four-switch buck-boost, (b) dual active bridge

converters is analyzed. Afterward, the simulation results are depicted in section IV. Finally, section V concludes the paper and presents an outlook on possible future research questions.

II. DC-DC CONVERTER

The specifications for the design of power converters are high power efficiency, low short circuit fault current, fast tuning performances avoiding large passive storage components and low current ripple avoiding component damage and ageing. This paragraph is going to introduce the basic theory of FSBB and DAB, in order to clarify the following analysis. Both converters have the capability of bidirectional power flow, which is very useful for ESSs and vehicle to grid (V2G) applications. They are particularly convincing due to their high power density, which allows practical uses of this converters also for on-board battery chargers of electric vehicles.

A. Four-Switch bidirectional Buck-Boost Converter

The idealized circuit diagram of a Four-Switch bidirectional Buck-Boost converter is shown in Fig. 1a. It is a non-isolated converter which benefits from a low number of switching elements and a simple design and control. With D_1 as the duty cycle of S_1 (while $S_2 = \overline{S_1}$) and D_2 as the duty cycle of S_4 (while $S_3 = \overline{S_4}$) the voltage gain of the FSBB can be expressed with [11]:

$$\frac{V_{DC2}}{V_{DC1}} = \frac{D_1}{1 - D_2} \quad (1)$$

The FSBB can be used in buck, boost, or buck-boost mode. From the ratio (1) it can be derived that if D_2 tends to zero the FSBB gets Buck property, whereas it gets Boost property for D_1 tending to zero. In this paper, the FSBB is used in Buck and boost modes by respectively setting $D_2 = 0$ and $D_1 = 1$. It allows also a current flow directly from one side to the other by simultaneously setting $D_1 = 1$ and $D_2 = 0$.

B. Dual Active Bridge Converter

DAB is one of the most widespread converters in DC microgrids and automotive applications. Even though it was firstly proposed in the early 1990s [12], losses due to old technologies of power devices resulted in low efficiency. However, it gained popularity after the development of silicon carbide (SiC) and gallium-nitride (GaN) switching devices [13], making it appealing for power grid applications. The

features that make this converter so appealing are the galvanic isolation, wide voltage gain range, and capability to perform soft-switching through proper modulation techniques [8], [9], [13].

As shown in Fig. 1b, the Dual Active Bridge is composed of two full bridges, connected to two voltage sources. This is a typical case of a ESSs connected to a DC grid through a medium or high frequency transformer to guarantee the galvanic isolation. The inductor L is modeled in series to the transformer and represents the sum of the leakage inductance of the transformer and an external inductor, which is designed to achieve a certain power transfer. The phase shift angle between the gate control signals of the two full bridges is used to regulate the power transfer of this converter, which can be described by:

$$P_{DAB} = \frac{nV_{DC1}V_{DC2}\varphi(\pi - |\varphi|)}{2f_s\pi^2L}, \quad \forall -\pi \leq \varphi \leq \pi \quad (2)$$

where n is the turn ratio N_1/N_2 and f_s is the switching frequency. The total inductance of the converter can be designed from (2) by imposing a maximum power transfer and a maximum phase shift angle.

C. Converter Losses

In this section, the loss analysis for both converters is performed. During the switching process of a SiC-MOSFET, energy losses occur due to the simultaneous presence of drain-source voltage and drain current. These losses are called switching losses. Due to the approximately triangular rise and fall of the drain-source voltage, the switch energy losses can be approximated by:

$$P_s = \frac{1}{2}V_{DS}I_D(t_r + t_f)f_s \quad (3)$$

where V_{DS} is the drain-source voltage and I_D is the RMS value of the drain current. Conduction losses in switching components can be modeled with an equivalent series resistance R_{on} . Hence, the conduction losses can be calculated with:

$$P_{cond,on} = R_{on}I_D^2 \quad (4)$$

where R_{on} is the equivalent series resistance of semiconductor. To prevent a short circuit of two series SiC-MOSFETs, a dead time t_{Dead} is used between the turn-on and the turn-off of the two switches respectively of the same leg. During this time the

current forced by the inductance flows through the body diode of the low-side SiC-MOSFET. The dead time losses P_{Dead} is calculated as:

$$P_{dead} = V_{diode} I_{diode} t_{dead} f_s \quad (5)$$

where V_{diode} is the forward voltage of the diode and I_D is the RMS value of the diode current. The inductor contributes essentially with conduction losses, converting electrical energy into heat due to the inductor resistive behavior. To represent these losses, a series DC resistance R_L has been modeled and hence calculated with:

$$P_L = R_L I_L^2 \quad (6)$$

where I_L is the RMS value of the inductor current. The capacitor losses, caused by leakage and dielectric loss, can also be modeled with an equivalent series resistance R_C and calculated in the same way as for inductor conduction loss in (6). Finally, the transformer losses for the DAB can also be modeled with a series resistance R_T , neglecting the magnetic losses. The total power loss will be modeled as a superposition of the aforementioned losses. The efficiency can thus be described according to the equation (7).

$$\eta = \frac{P_{out}}{P_{In}} = \frac{P_{out}}{P_{out} + \sum(P_s + P_{cond,on} + P_{dead}) + P_R} \quad (7)$$

where P_R is the sum of the resistor losses related to inductors, capacitors and transformer.

III. SHORT-CIRCUIT ANALYSIS

A. Four-Switch Buck-Boost

Depending on the converter type and mode, there are multiple different impacts on the DC fault characteristic. In boost mode three causes contribute to the short circuit current. The natural discharging response occurring from the capacitors, inductor forced current through the freewheeling diodes, and the input source feeding through the diodes [2]. The capacitor discharge current occurs through the RC circuit and can be written as:

$$R_{fault} \frac{di_{fault,C}(t)}{dt} + \frac{1}{C} i_{fault,C}(t) = 0 \quad (8)$$

The equation (8) can be used for Boost as well as for buck mode and also for short circuit analysis on each side. While the boost mode has a natural response coming from the capacitors, the freewheeling diodes, and the input source feeding, the buck mode has an intrinsic immunity to the input source impacts [2], [14]. Consequently, a FSBB has the ability to prevent input source influence in case of a high voltage side short circuit. The freewheeling current differs depending on the short circuit side. In both cases, the current can be calculated with the discharge function of a RL-circuit.

$$L \frac{di_{fault,L}(t)}{dt} + (R_L + R_{fault}) i_{fault,L}(t) = 0 \quad (9)$$

Without an additional safety mechanism in boost mode operation, the fault current will increase to the system limits

[2], [14]. Since a short circuit on the high voltage side will cause the voltage to zero, the FSBB will change to buck mode and consequently, it will be able to suppress the current through the converter. The short circuit behavior after switching to buck mode will also depend on the control algorithm. The investigation of control effects to short circuit behavior is not part of this paper.

B. Dual Active Bridge

The short circuit dynamic of the DAB has been already discussed in [15]. It can be carried on by neglecting the dynamic of the capacitor on the first side of the DAB and considering a fault resistance R_{fault} . This results in two differential equations, of which the first one describes the inductor's current behavior:

$$\frac{di_L(t)}{dt} = \frac{V_{dc1}}{L} M_1(t) - \frac{N_1}{N_2} \frac{v_2(t)}{L} M_2(t) - \frac{R_L}{L} i_L(t). \quad (10)$$

The second one rather describes the voltage of the capacitor on the second side of the converter:

$$\frac{dv_2(t)}{dt} = \frac{N_1}{N_2} \frac{i_L(t)}{C_o} M_2(t) - \frac{v_2(t)}{R_{fault} C_o}, \quad (11)$$

where $M_1(t)$ and $M_2(t)$ are the modulation functions, obtained as:

$$M_1(t) = D_1(t) - D_2(t) \quad (12)$$

$$M_2(t) = D_3(t) - D_4(t) \quad (13)$$

An equivalent simplified model of DAB for first side faults can be obtained by neglecting the second side capacitor and inserting R_{fault} on the first side instead.

Moreover, the steady state behaviour of this converter in the phasor domain has been investigated in [16]. Here, it is supposed that the switching devices can tolerate up to two times their rated current and after a mathematical analysis it was obtained that the inductor must be designed for a phase shift $28.96^\circ \leq \varphi \leq 90^\circ$.

IV. SIMULATION RESULTS AND COMPARISON

This section evaluates the short circuit performances and efficiency results for both converters by using the Matlab/Simulink environment. The specifications of the converters are reported in Tab. I and II, in which it is possible to notice that the first and secondary voltages are respectively $V_{DC1} = 400$ V and $V_{DC2} = 750$ V, whereas the power rating is $P = 5$ kW. These power and voltage ratings are typical of home electric vehicle battery charger applications. In the following simulations, the efficiency has been evaluated from 1% to 100% at 1% steps, whereas the short circuit fault has been simulated at $t_{fault} = 0.1$ s.

A. Efficiency simulation results

Fig. 2 shows the simulated converter efficiency as a function of output power in percentage up to 5 kW at 100%. The FSBB

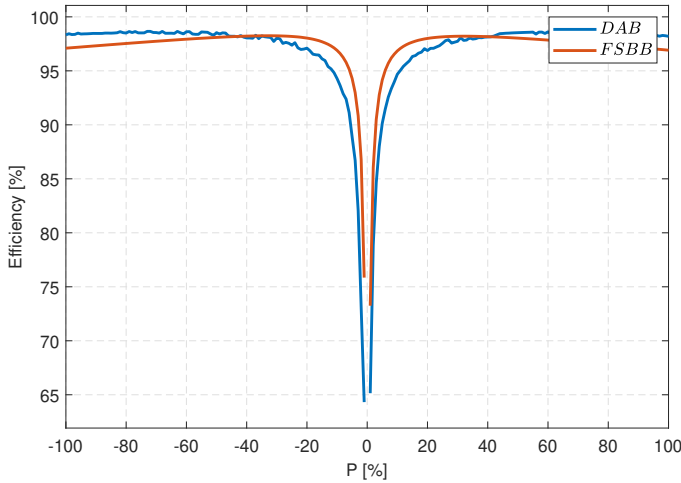
TABLE I: System specification

System Parameters			
Name	Value	Name	Value
P	5 kW	C_1	235 μF
f_{sw}	20 kHz	C_2	235 μF
V_{DC1}	400 V	L_{DAB}	177.78 μH
V_{DC2}	750 V	L_{FSBB}	5.5 mH

TABLE II: Losses specification

Loss Parameters			
Name	Value	Name	Value
t_r	22 ns	R_{on}	80 m Ω
t_f	14 ns	R_{C1}	0.02 Ω
t_{dead}	150 ns	R_{C2}	0.02 Ω
$R_{L_{FSBB}}$	0.3 Ω	$R_{L_{DAB}}$	0.03 Ω

achieves a peak efficiency of 98.25 % at 32 % of the maximum power considered. On the other hand, the DAB reaches a peak efficiency of 98.66 % at 73 % of the maximum power. The DAB efficiency surpasses the efficiency of the FSBB converter at 41 % of the maximum power. A comparison of the simulated results for the converter efficiencies shows that FSBB has a higher efficiency in low power ranges, whereas DAB has a higher efficiency in high power ranges.


 Fig. 2: Efficiency from -5 kW to $+5$ kW for DAB and FSBB

B. DC fault results for the Four-Switch Buck-Boost

Since an FSBB converter is only meaningful in combination with a mode switching control, the following simulations are performed using a simple mode switch. Depending on the voltage level of both sides, switching between buck and boost mode is performed. Fig. 3 shows the simulated transient behavior of a FSBB with a short circuit fault at $t_{fault} = 0.1$ s. Fig. 3a depicts that the main contribution to the fault current is coming from the capacitor discharge current in the form of an exponential fall according to (8). In Fig. 3b a suppression

of the HV side current is noticeable. For the short circuit fault on the HV side, the simulation results are illustrated in Fig. 4. It is worth highlighting that the contribution of the LV side in the case of a short circuit fault on the HV side is restricted as exposed in Fig. 4a. Unlike the conventional boost converter, the FSBB is able to suppress the fault current on the LV side in the case of a short circuit on the HV side. The short circuit fault will drop the voltage on the HV side down, which will lead to a switch of the FSBB to buck mode. The spikes in Fig. 3b and 4a result from the fact that the reference current value through the converter is 6.6 A. The control algorithm is switching the SiC-MOSFETs on to reach the reference.

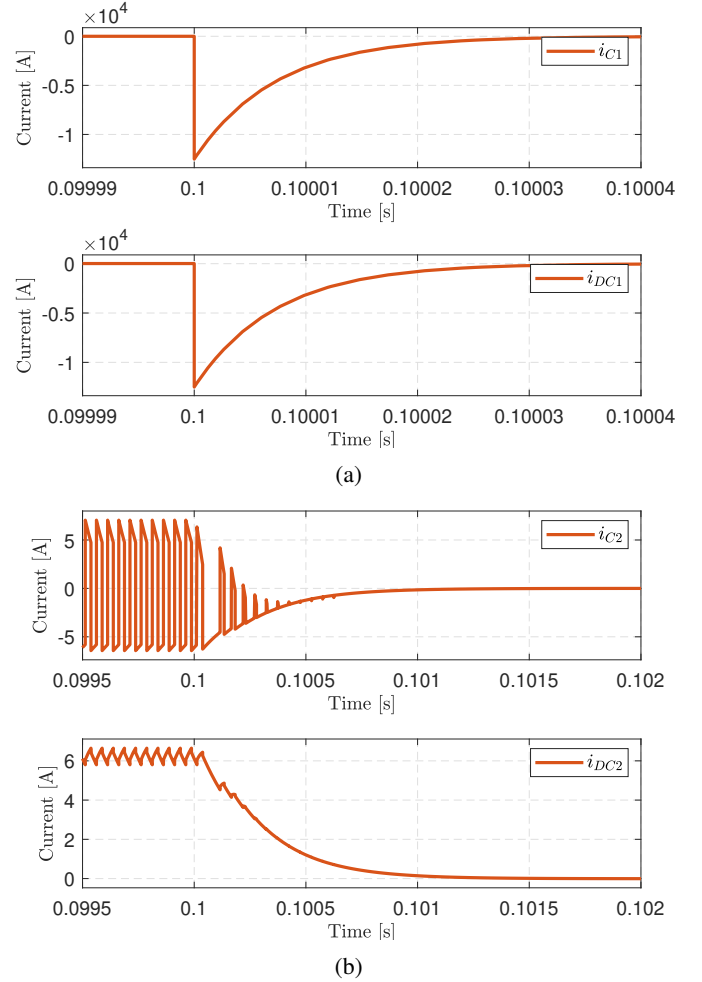


Fig. 3: Transient behavior of the FSBB during LV fault: a) LV side capacitor current and DC current, b) HV side capacitor current and DC current

C. DC fault results for the Dual Active Bridge

The DAB converter has been designed for a maximum phase shift of 60° at the maximum power of 5 kW, since the maximum phase shift angle of 90° is usually avoided for control reasons during normal operations. The short circuit simulations have been carried out in open loop to show the ability of this converter to work during faults. The related

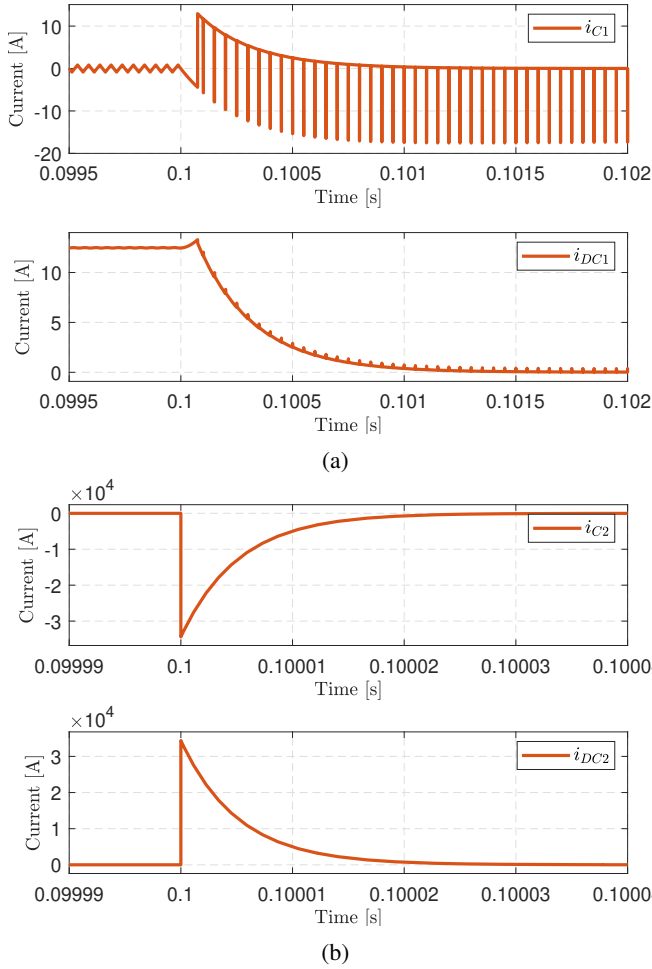


Fig. 4: Transient behavior of the FSBB during HV fault: a) LV side capacitor current and DC current, b) HV side capacitor current and DC current

results of LV and HV faults are shown in Fig. 5 and 6, where it is possible to notice that the main contribution of the fault current comes from the capacitor. Moreover, DAB is able to nullify its fault current contributions in milliseconds range, as shown in Fig. 5b and 6a. Further fault riding-through strategies can be used to improve DAB performances in faulty conditions, such as blocking the switching signals or adding a proper inductor on the output terminals to limit the fault current as described in [15].

D. Comparison of the short circuit behavior

Simulations show that the main contribution to the short circuit current of both converters comes from the filter capacitors. Since DC Microgrids require this kind of filters to correctly operate, it is not possible to eliminate this problem, which increases in high power applications due to the increased size of capacitors. DAB and FSBB demonstrated an inherent capability to suppress the fault current in milliseconds range for both LV and HV faults. In particular, FSBB needs a mode switch mechanism to prevent the fault current to grow

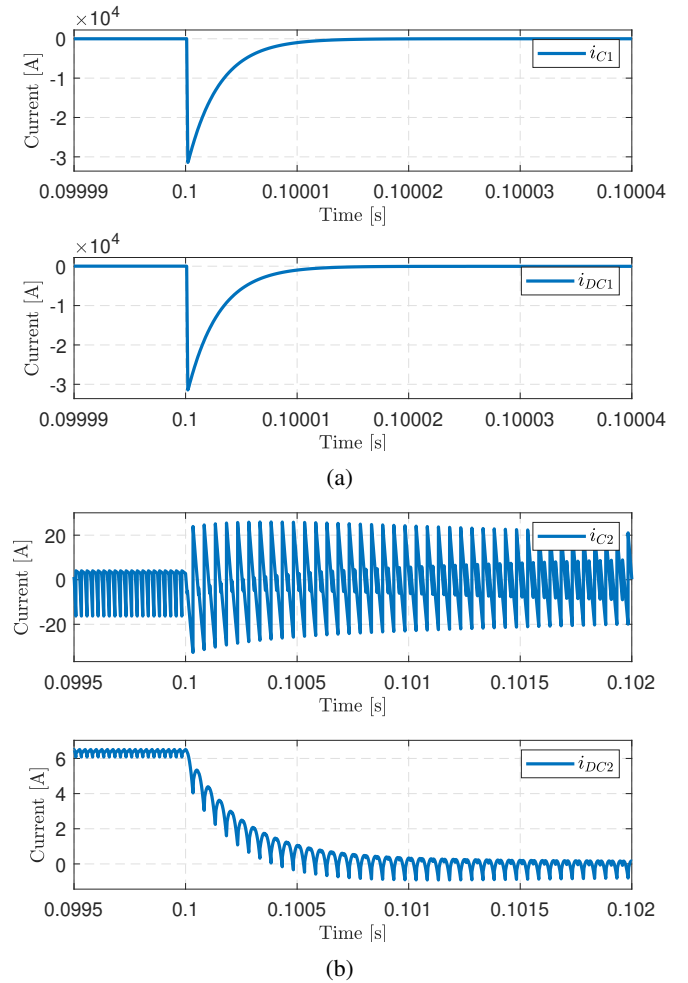


Fig. 5: Transient behavior of the DAB during LV fault: a) LV side capacitor current and DC current, b) HV side capacitor current and DC current

exponentially, which makes this converter not robust in case of controller malfunctioning or measurement failure. On the other side, DAB is intrinsically safe even without any control strategy to bring the fault current to zero, because of the galvanic isolation provided by its transformer.

V. CONCLUSION AND OUTLOOK

This paper compares the FSBB and the DAB regarding their efficiency and their short circuit behavior. It has been shown that for both converters the largest contribution results from the discharge of the capacitors. The simulation results have confirmed the possibility of decoupling the input and output sides after short circuit faults for both converters. While the galvanic isolation of the DAB provides an intrinsic short circuit decoupling of both sides, the FSBB needs a mode switch mechanism to change into buck mode in case of a voltage drop while the short circuit occurs. The efficiency simulation has shown that the FSBB is significantly more efficient than a DAB in the low power conversion range, on the other hand, the DAB efficiency surpasses in the high power

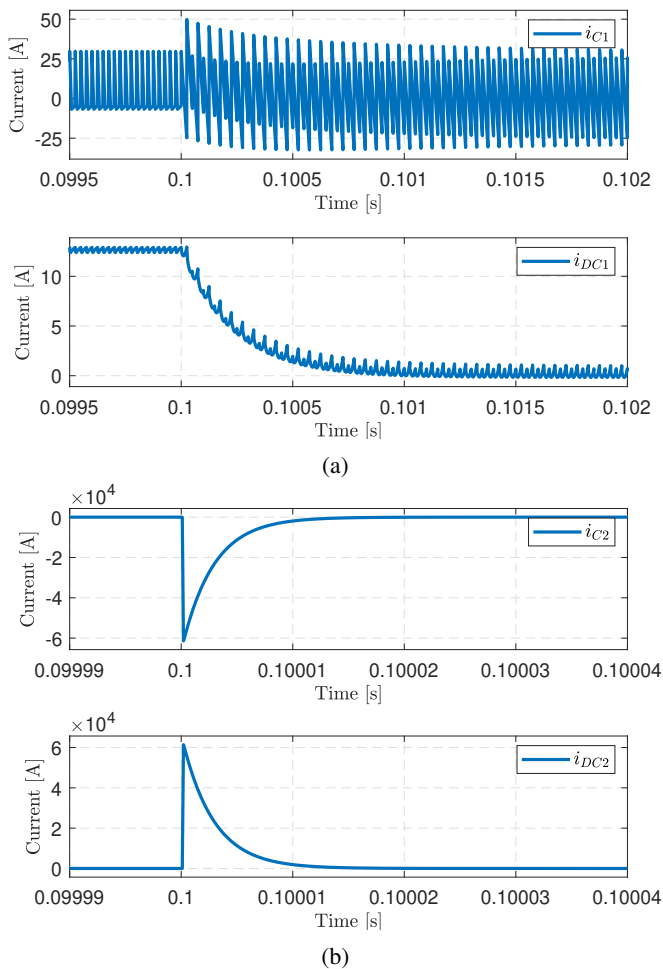


Fig. 6: Transient behavior of the DAB during HV fault: a) LV side capacitor current and DC current, b) HV side capacitor current and DC current

conversion range. Depending on the intended application the choice of FSBB could lead to better efficiency for components that have a low power transmission in their steady state. For DC Microgrid components that mainly absorb and release high power, the DAB could lead to efficiency improvement.

REFERENCES

- [1] D. Kumar, F. Zare and A. Ghosh, "DC Microgrid Technology: System Architectures, AC Grid Interfaces, Grounding Schemes, Power Quality, Communication Networks, Applications, and Standardizations Aspects," in *IEEE Access*, vol. 5, pp. 12230-12256, 2017, doi: 10.1109/ACCESS.2017.2705914.
- [2] S. Beheshtaein, R. M. Cuzner, M. Forouzesh, M. Savaghebi and J. M. Guerrero, "DC Microgrid Protection: A Comprehensive Review," in *IEEE Journal of Emerging and Selected Topics in Power Electronics*, March 2019, doi: 10.1109/JESTPE.2019.2904588.
- [3] S. A. Gorji, H. G. Sahebi, M. Ektesabi and A. B. Rad, "Topologies and Control Schemes of Bidirectional DC-DC Power Converters: An Overview," in *IEEE Access*, vol. 7, pp. 117997-118019, 2019, doi: 10.1109/ACCESS.2019.2937239.
- [4] Q. Liu, Q. Qian, M. Zheng, S. Xu, W. Sun and T. Wang, "An Improved Quadrangle Control Method for Four-Switch Buck-Boost Converter With Reduced Loss and Decoupling Strategy," in *IEEE Transactions*

- on *Power Electronics*, vol. 36, no. 9, pp. 10827-10841, Sept. 2021, doi: 10.1109/TPEL.2021.3064074.
- [5] L. Callegaro, M. Ciobotaru, D. J. Pagano and J. E. Fletcher, "Feedback Linearization Control in Photovoltaic Module Integrated Converters," in *IEEE Transactions on Power Electronics*, vol. 34, no. 7, pp. 6876-6889, July 2019, doi: 10.1109/TPEL.2018.2872677.
- [6] C. Chen, K. Chen and Y. Chen, "Modeling and Controller Design of an Autonomous PV Module for DMPPT PV Systems," in *IEEE Transactions on Power Electronics*, vol. 29, no. 9, pp. 4723-4732, Sept. 2014, doi: 10.1109/TPEL.2013.2287752.
- [7] G. Arena, G. Aiello, G. Scelba, M. Cacciato and F. Gennaro, "A Cost-Effective Hardware in the Loop Implementation of Dual Active Bridge for Fast Prototyping of Electric Vehicles Charging Controls," 2021 23rd European Conference on Power Electronics and Applications (EPE'21 ECCE Europe), 2021, pp. P.1-P.10.
- [8] F. Krismer and J. W. Kolar, "Accurate Small-Signal Model for the Digital Control of an Automotive Bidirectional Dual Active Bridge," in *IEEE Transactions on Power Electronics*, vol. 24, no. 12, pp. 2756-2768, Dec. 2009, doi: 10.1109/TPEL.2009.2027904.
- [9] S. Shao et al., "Modeling and Advanced Control of Dual-Active-Bridge DC-DC Converters: A Review," in *IEEE Transactions on Power Electronics*, vol. 37, no. 2, pp. 1524-1547, Feb. 2022, doi: 10.1109/TPEL.2021.3108157.
- [10] S. P. Engel, M. Stieneker, N. Soltan, S. Rabiee, H. Stagge and R. W. De Doncker, "Comparison of the Modular Multilevel DC Converter and the Dual-Active Bridge Converter for Power Conversion in HVDC and MVDC Grids," in *IEEE Transactions on Power Electronics*, vol. 30, no. 1, pp. 124-137, Jan. 2015, doi: 10.1109/TPEL.2014.2310656.
- [11] M. Orellana, S. Petibon, B. Estivals and C. Alonso, "Four Switch Buck-Boost Converter for Photovoltaic DC-DC power applications," *IECON 2010 - 36th Annual Conference on IEEE Industrial Electronics Society*, 2010, pp. 469-474, doi: 10.1109/IECON.2010.5674983.
- [12] R. W. A. A. De Doncker, D. M. Divan and M. H. Kheraluwala, "A three-phase soft-switched high-power-density DC/DC converter for high-power applications," in *IEEE Transactions on Industry Applications*, vol. 27, no. 1, pp. 63-73, Jan.-Feb. 1991, doi: 10.1109/28.67533.
- [13] B. Zhao, Q. Song, W. Liu and Y. Sun, "Overview of Dual-Active-Bridge Isolated Bidirectional DC-DC Converter for High-Frequency-Link Power-Conversion System," in *IEEE Transactions on Power Electronics*, vol. 29, no. 8, pp. 4091-4106, Aug. 2014, doi: 10.1109/TPEL.2013.2289913.
- [14] Shulin Liu, Jian Liu, Yinling Yang and Jiuming Zhong, "Design of intrinsically safe buck DC/DC converters," 2005 International Conference on Electrical Machines and Systems, 2005, pp. 1327-1331 Vol. 2, doi: 10.1109/ICEMS.2005.202763.
- [15] Y. Chen and Y. Zhang, "Fault Characteristics and Riding-Through Methods of Dual Active Bridge Converter Under Short-Circuit of the Load," in *IEEE Transactions on Power Electronics*, vol. 36, no. 8, pp. 9578-9591, Aug. 2021, doi: 10.1109/TPEL.2021.3054023.
- [16] M. I. Rahman, K. H. Ahmed and D. Jovcic, "Analysis of DC Fault for Dual-Active Bridge DC/DC Converter Including Prototype Verification," in *IEEE Journal of Emerging and Selected Topics in Power Electronics*, vol. 7, no. 2, pp. 1107-1115, June 2019, doi: 10.1109/JESTPE.2018.2856759.